

Projected constraints on the dispersion of gravitational waves using advanced ground- and space-based interferometers

Anuradha Samajdar^{1,*} and K. G. Arun^{2,3,†}

¹*IISER-Kolkata, Mohanpur, West Bengal 741252, India*

²*Chennai Mathematical Institute, Siruseri, 603103 India*

³*Institute for Gravitation and the Cosmos, Pennsylvania State University, State College, PA 16802*

(Dated: July 6, 2021)

Certain alternative theories of gravity predict that gravitational waves will disperse as they travel from the source to the observer. The recent binary black hole observations by Advanced-LIGO have set limits on a modified dispersion relation from the constraints on their effects on gravitational-wave propagation. Using an identical modified dispersion, of the form $E^2 = p^2 c^2 + \mathbb{A} p^\alpha c^\alpha$, where \mathbb{A} denotes the magnitude of dispersion and E and p are the energy and momentum of the gravitational wave, we estimate the projected constraints on the modified dispersion from observations of compact binary mergers by third-generation ground-based detectors such as the Einstein Telescope and Cosmic Explorer as well as the space-based detector Laser Interferometer Space Antenna. We find that third-generation detectors would bound dispersion of gravitational waves much better than their second-generation counterparts. The Laser Interferometer Space Antenna, with its extremely good low-frequency sensitivity, would place stronger constraints than the ground-based detectors for $\alpha \leq 1$, whereas for $\alpha > 1$, the bounds are weaker. We also study the effect of the spins of the compact binary constituents on the bounds.

I. INTRODUCTION

The direct detection of gravitational waves (GWs) by the LIGO and Virgo collaborations [1–4] are giving us the first glimpses of the strong-field dynamics associated with the mergers of binary black holes. We now have the first constraints on the deviation from the post-Newtonian coefficients [3–11], mass of the graviton [3, 4, 11–13], and consistency between inspiral and merger-ringdown phases of the binary evolution [3, 4, 11, 14]. The latest addition to the set of tests is the constraint on the possible dispersion of gravitational waves [4, 15, 16]. If the propagating GWs disperse, then the dispersion will lead to dephasing of the GW signal [15, 16]. The consistency of the observed phase with that of general relativity (GR) will hence set limits on possible dispersion. The results for the constraints on modified dispersion, from the three binary black hole (BBH) detections, are presented in Fig. 5 of Ref.[4]. While these bounds are the first from the gravity sector for superluminal propagation of GWs, the bounds from gravitational Cherenkov radiation (though very much model dependent) are better than these for subluminal propagation [17–19].

One natural way to invoke dispersion of GWs is to postulate that the underlying theory of gravity does not respect local Lorentz invariance, one of the fundamental pillars of GR. Hence, the bounds on dispersion can be translated to constraints on parameters of Lorentz violating theories of gravity [16]. Using GW150914, the first BBH detected by LIGO, Ref. [20] discusses constraints on the Standard Model extension, a generic framework to model Lorentz violating theories of gravity [21, 22]. The accuracy on the delay time between the two LIGO detectors was used to constrain the speed of GW using GW150914 in Refs. [23, 24]. Using the inferred parameters and constraints on the post-Newtonian phasing coefficients of GW150914 and GW151226 [3, 11], Ref. [16] discusses the bounds on possible Lorentz violation.

Improved sensitivities of next generation ground- and space-based detectors can significantly improve these bounds, possibly ruling out certain classes of alternative theories of gravity which predict dispersion of GWs. This forms the theme of this paper in which we obtain the projected bounds on constraining modified dispersion of GWs using third-generation (3G) ground-based detectors such as Einstein Telescope (ET) [25] and Cosmic Explorer (CE) [26] as well as the space-based detector Laser Interferometer Space Antenna LISA [27], expected to be launched in the early 2030s, preparations for which are underway.

Such investigations have been carried out in the past by several authors. Following the proposal by Will [12], constraints on the mass of the graviton using advanced ground- and space-based detectors were studied in Refs. [12, 13, 28] using post-Newtonian gravitational waveforms that account for the inspiral phase of the binary evolution. Using analytical waveforms that extend beyond inspiral and account for the merger and ringdown of the binary, Keppel and Ajith [29] carried out a similar study for the bounds on graviton mass using advanced GW detectors for nonspinning systems. Mirshekari *et al.* [15] proposed an extension of this idea to include dispersion relations that include Lorentz violation (which is what we follow here) and deduced the bounds on the modified dispersion using nonspinning post-Newtonian waveforms [30, 31]. Reference [32] discussed bounds on Lorentz violating theories of gravity using GW observations with and without electromagnetic counterparts.

*Electronic address: anuradha1115@iiserkol.ac.in

†Electronic address: kgarun@cmi.ac.in

A recent study by Chamberlain and Yunes [33] made a detailed analysis of the improvement on the constraints on several alternative theories of gravity from advanced ground- and space-based GW detectors. Using the parametrized post-Einsteinian formalism [8], they studied systems similar to the gravitational signal GW150914 as well as other canonical binary black holes for ground-based detectors and binaries involving supermassive black holes for space-based detectors. Amongst others, the alternatives include the presence of a massive graviton in the GW dispersion relation and specific Lorentz violating theories, namely, the Einstein-Aether and the khronometric theories. They used propagation effects at the first post-Newtonian order to derive the mass of the graviton, while correction to the Newtonian GW phasing was used to put bounds on certain Lorentz violating theories of gravity.

In this work, we consider more realistic waveforms that account for inspiral, merger, and ringdown phases as well as study the effect of the presence of spins. We extend the analysis to include generic dispersion and derive bounds on the magnitude of dispersion for different types of modifications and for different detector sensitivities. Our goal here is to discuss the ability of advanced detectors to constrain the possible dispersion of GWs without referring to any particular theory of gravity. We consider only propagation effects here as our aim is to probe dispersion.

The rest of the paper is organized as follows. Section II describes the modified dispersion relation and the expression for a resulting dephasing of the gravitational waves. We introduce the waveform, detector sensitivities, and Fisher matrix formalism in Sec. III. The results and conclusions are discussed in Sec. IV, and conclusions and outlook are presented in Sec. V.

II. CONSTRAINING DISPERSION OF GRAVITATIONAL WAVES

Following Refs. [15, 16], we consider a modified dispersion relation for GWs, which is given by

$$E^2 = p^2 c^2 + \mathbb{A} p^\alpha c^\alpha, \quad (2.1)$$

where E and p are the energy and momentum of GWs and \mathbb{A} denotes the magnitude of dispersion corresponding to the exponent α . As shown in Ref. [15], this modified dispersion relation leads to a dephasing of the gravitational signal given, in the frequency domain, by

$$\Psi_{\text{total}}(f) = \begin{cases} \Psi_{\text{GR}}(f) - \zeta u^{\alpha-1} & \alpha \neq 1, \\ \Psi_{\text{GR}}(f) + \zeta \ln u & \alpha = 1. \end{cases} \quad (2.2)$$

In the above, $u = (\pi \mathcal{M} f)$, where \mathcal{M} is the chirp mass of the binary and f is the GW frequency. ζ is given by

$$\zeta = \begin{cases} \frac{\pi^{2-\alpha}}{(1-\alpha)} \frac{D_\alpha}{\lambda_\Lambda^{2-\alpha}} \frac{\mathcal{M}^{1-\alpha}}{(1+z)^{1-\alpha}} & \alpha \neq 1, \\ \frac{\pi D_1}{\lambda_\Lambda} & \alpha = 1, \end{cases} \quad (2.3)$$

where $\lambda_\Lambda \equiv hc\mathbb{A}^{\frac{1}{\alpha-2}}$ (with c and h referring to the speed of light and Planck constant, respectively) denotes the length scale introduced by the dispersion and

$$D_\alpha = \frac{(1+z)^{1-\alpha}}{H_0} \int_0^z \frac{(1+z')^{\alpha-2}}{\sqrt{\Omega_m(1+z')^3 + \Omega_\Lambda}} dz', \quad (2.4)$$

is a distance measure introduced by dispersion.

Ω_m and Ω_Λ are, respectively, the matter and dark energy fractions in a (flat) Λ_{CDM} model of cosmology, for which we use the values (0.3065, 0.6935) estimated by the Planck Collaboration [34].

The group velocity of GWs, with the modified dispersion relation, can easily be obtained by differentiating it with respect to p , which to the leading order in $\mathbb{A}E^{\alpha-2}$, reads $v_{\text{gw}} = c \left(1 + \frac{\alpha-1}{2} \mathbb{A} E^{\alpha-2}\right)$. Depending on the sign of \mathbb{A} and the value of α , GWs may propagate superluminally or subluminally. The bounds from GW observations, reported in Ref.[4], have been derived for both these sectors (see Fig. 5 of Ref.[4]). However, using the parameter estimation method that we employ here, we cannot obtain bounds for these two sectors separately.

Since the method explored here is generic, α can take any value greater than or equal to 0, depending on the alternative theory. Here, we consider the representative cases of $\alpha = 0, 1, 2.5, 3$. The $\alpha = 0$ bounds can easily be mapped onto a bound on graviton mass (assuming $\mathbb{A} > 0$). The $\alpha = 1$ modification, as can be seen from Eq. (2.3), is a special case that brings in logarithmic correction to the GR phasing. Modifications with $\alpha = 2.5$ and $\alpha = 3$ correspond to certain Lorentz violating alternative theories of gravity such as multifractal spacetime [35] and doubly special relativity [36], respectively.

The goal of this paper is to calculate the projected accuracy with which the magnitude of dispersion parameter \mathbb{A} can be bounded by future observations of compact binaries by advanced ground- and space-based detectors, as a function of the total mass of the compact binaries for different values of α . Dimensionally, \mathbb{A} (for a given α) has the unit of energy $^{2-\alpha}$, and hence our bounds are reported in units of eV $^{2-\alpha}$, a convenient unit for all α . These bounds are obtained by using the expected sensitivities of the future GW detectors and using the parameter estimation technique of Fisher information matrix where the compact binary waveforms will be modeled by the IMRPhenomB model restricting to equal-mass binary black hole mergers (which will be representative of the typical bounds even for asymmetric binaries).

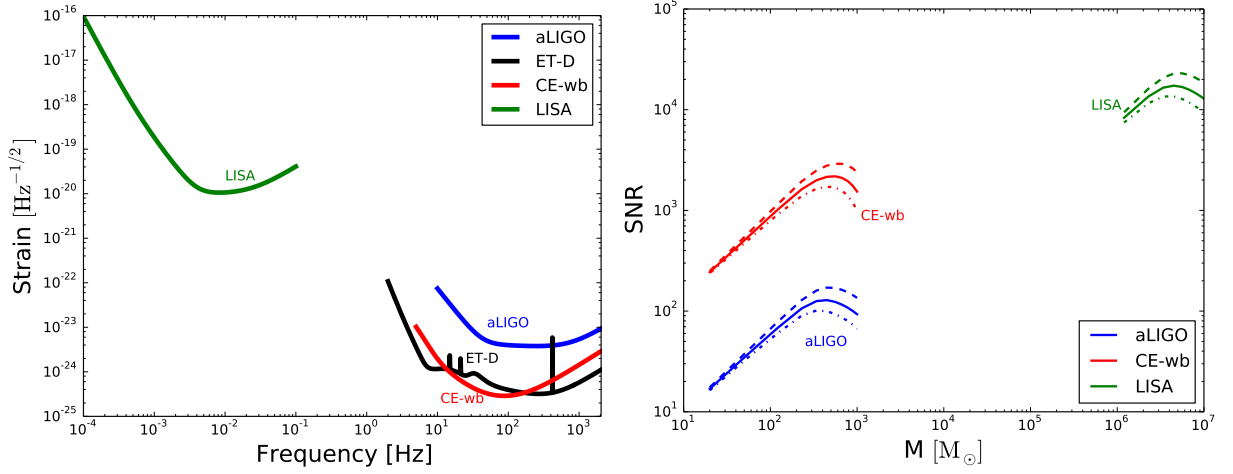


FIG. 1: Strain sensitivities of ET-D (black curve), CE-wb (red curve), aLIGOZeroDetHighPower (blue curve), and LISA (green curve) overlaid. The corresponding signal-to-noise ratios as a function of the total mass of the compact binary are on the right panel. The sources considered consist of nonspinning (solid curves), with $\chi = 0.4$ (dashed curves) and with $\chi = -0.4$ (dash-dotted curves). The sources targeted by CE, aLIGO, and ET are at a redshift of 0.2, and the LISA sources are at a redshift of 0.5.

III. ANALYSIS SET UP

A. Waveform model

We use the analytical waveform model IMRPhenomB [37] as an example of a gravitational waveform containing the inspiral, merger, and ringdown phases of the binary's evolution. This waveform family is obtained by combining the post-Newtonian description [30, 31, 38] of the inspiral with a set of numerical relativity simulations (up to a mass ratio of 4) accounting for spin effects when the spins are (anti)aligned with respect to the orbital angular momentum vector of the binary. A more recent family of waveforms, IMRPhenomD [39], is calibrated to numerical simulations with higher mass ratios up to 18. However, we focus on equal-mass systems for which the two waveforms do not differ significantly. The definition of χ in the above equation depends on the two component masses m_1 and m_2 and the corresponding dimensionless spin parameters χ_1 and χ_2 where $\chi_1 \equiv \frac{|S_1|}{m_1^2}$ and similarly for χ_2 . Schematically, the waveform reads

$$\tilde{h}(f) = C \mathcal{B}(f; M, \eta, \chi) e^{i\Psi(f; M, \eta, \chi)}, \quad (3.1)$$

where M is the total mass, η the symmetric mass ratio and χ is the effective spin parameter. C encodes information about the luminosity distance, source location, and orientation, whereas \mathcal{B} contains the dependences on the intrinsic parameters (masses and spins). The exact waveform we use is given in Eq. 1 and Table I of Ref.[37]. The waveform is truncated at the frequency referred to as f_3 (and given in Table 1) of Ref.[37]. The phase of the IMRPhenomB waveform is deformed accounting for GW dispersion following Eq. (2.2).

B. Sensitivity of future detectors

The detector noise is modeled as a stationary, zero-mean Gaussian, random process. The assumption of stationarity implies that the noise properties do not change over time. If $\tilde{n}(f)$ is the Fourier transform of the noise $n(t)$, the noise power spectral density (PSD) $S_h(f)$ is defined by

$$\langle \tilde{n}(f) \tilde{n}^*(f') \rangle = \frac{1}{2} S_h(f) \delta(f - f'), \quad (3.2)$$

where δ denotes the Dirac delta function. In this section, we list the sensitivities of different detector configurations we use in the present work: the ET, CE, and LISA. For comparison of results, we also list the design sensitivity of advanced LIGO detector.

1. Design sensitivity of AdvLIGO

An analytic fit to Advanced LIGO's zero-detuned-high-power (called aLIGOZeroDetHighPower) PSD is given in Ref. [40] as

$$S_h(f) = 10^{-48} (0.0152x^{-4} + 0.2935x^{9/4} + 2.7951x^{3/2} - 6.5080x^{3/4} + 17.7622) \text{ Hz}^{-1}, \quad (3.3)$$

where $x = f/245.4$. For the studies done with Advanced LIGO sensitivity below, we use a lower-frequency cutoff of 10 Hz.

2. Einstein Telescope

ET is an envisaged 3G detector with proposed frequency sensitivity in the range of $1 - 10^4$ Hz. Details of its sensitivity design are given by Hild *et al.* [41]. In the following study, we use the sensitivity of the ET-D configuration given in Ref. [42] with a 2 Hz lower-frequency cutoff.

3. Cosmic Explorer

Dwyer *et al.* [43] introduced the idea of a ground-based interferometer with an arm length of 40 km, which is referred to as CE. It has been argued that 40 km is the optimal arm length beyond which no additional scientific gain would be evident. Various noise sources corresponding to CE are also discussed by Abbott *et al.* [26], from which we have used an analytical fit to the CE-wb configuration [44] given by

$$S_h(f) = 10^{-50} (11.5f_{10}^{-50} + f_{25}^{-10} + f_{53}^{-4} + 2f_{80}^{-2} + 5 + 2f_{100}^2) \text{ Hz}^{-1}, \quad (3.4)$$

where $f_k \equiv (f/k)$ Hz. In the following discussion, we shall mean the CE-wb configuration when we refer to the CE sensitivity. We use a low-frequency cutoff of 5 Hz for our studies below.

4. LISA

LISA was proposed as a space-based GW observatory sensitive to a frequency range $\sim 10^{-4} - 0.1$ Hz and capable of observing mergers of supermassive binary black holes with masses between $\sim 10^4 - 10^7 M_\odot$. There is increased enthusiasm about LISA after the promising scientific output from LISA Pathfinder [45]. We use the latest noise PSD of LISA used by Babak *et al.* [46] given by

$$S_h(f) = \frac{20}{3} \frac{4S_n^{acc}(f) + 2S_n^{loc} + S_n^{sn} + S_n^{omn}}{L^2} \times \left[1 + \left(\frac{2Lf}{0.41c} \right)^2 \right] \text{ Hz}^{-1}, \quad (3.5)$$

where L is the arm length, now considered to be 2.5×10^9 m, $S_n^{acc}(f)$, S_n^{loc} , S_n^{sn} , and S_n^{omn} are, respectively, the noise contributions due to the low-frequency acceleration, local interferometer noise, shot noise, and other measurement noise. The low-frequency noise is given by

$$S_n^{acc}(f) = \left\{ 9 \times 10^{-30} + 3.24 \times 10^{-28} \left[\left(\frac{3 \times 10^{-5} \text{ Hz}}{f} \right)^{10} + \left(\frac{10^{-4} \text{ Hz}}{f} \right)^2 \right] \right\} \left(\frac{1 \text{ Hz}}{2\pi f} \right)^4 \text{ m}^2 \text{ Hz}^{-1}. \quad (3.6)$$

The other noise components are given by

$$\begin{aligned} S_n^{loc} &= 2.89 \times 10^{-24} \text{ m}^2 \text{ Hz}^{-1}, \\ S_n^{sn} &= 7.92 \times 10^{-23} \text{ m}^2 \text{ Hz}^{-1}, \\ S_n^{omn} &= 4.00 \times 10^{-24} \text{ m}^2 \text{ Hz}^{-1}. \end{aligned} \quad (3.7)$$

Figure 1 shows the sensitivities of all configurations of the detectors used here.

C. Fisher Information Matrix

All analyses carried out here have been done with a Fisher matrix approach [47]. Assuming the noise in a GW detector to be Gaussian, the likelihood is given by

$$p(d|\vec{\theta}) = \exp \left[-\frac{1}{2} \Gamma_{ab} \Delta\theta^a \Delta\theta^b \right], \quad (3.8)$$

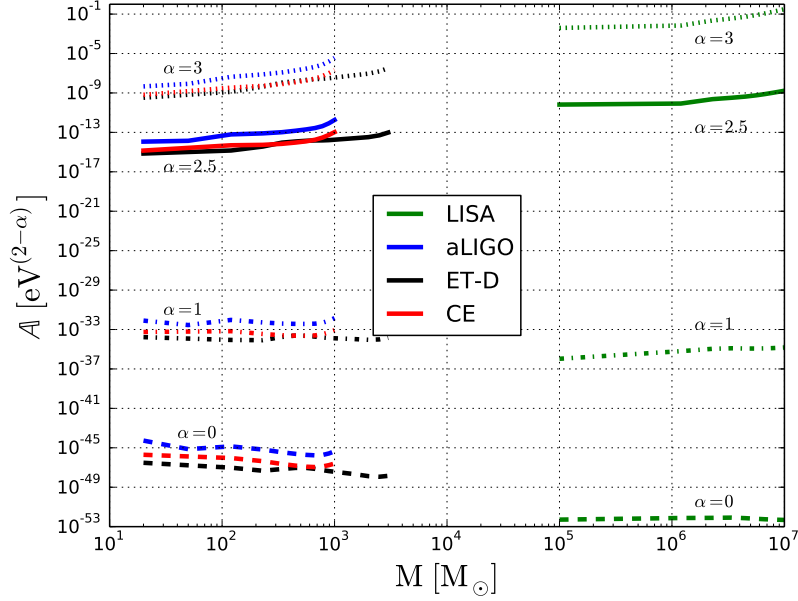


FIG. 2: Upper bounds on \mathbb{A} obtained with equal-mass nonspinning sources for future ground-based detectors and the planned space-based detector LISA. For ground-based detectors, we use the future design of aLIGO (in blue), the 3G detectors ET (in black) and CE (in red). The total masses vary from $20 - 1000 M_\odot$ for aLIGO and CE and lie between $20 - 3000 M_\odot$ for ET. The total masses vary between $10^5 - 10^7 M_\odot$ for sources targeted by LISA (in green). All bounds are obtained for $\alpha = 0$ (dashed lines), $\alpha = 1$ (dash-dotted lines), $\alpha = 2.5$ (solid lines) and $\alpha = 3$ (dotted lines). The sources targeted by the ground-based detectors are at a redshift of 0.2 and the LISA sources occur at a redshift of 0.5.

where Γ_{ab} denotes the Fisher information matrix and $\Delta\theta^a$ represents the error in estimation of the parameter θ^a .

$\Delta\theta^a$ is given by $\sqrt{\Sigma^{aa}}$, where Σ is the covariance matrix given by the inverse of the Fisher information matrix Γ . The diagonal elements of Σ represent the errors whereas the off-diagonal elements give us the correlation coefficients between the parameters. Components of the Fisher matrix are given by

$$\Gamma_{ab} = \left(\frac{\partial h}{\partial \theta^a} \middle| \frac{\partial h}{\partial \theta^b} \right), \quad (3.9)$$

where h is the waveform in frequency domain. The scalar product notation between two frequency domain waveforms h_1 and h_2 is defined as

$$(h_1|h_2) = 2\mathcal{R} \int_{f_{\text{low}}}^{f_{\text{high}}} \frac{h_1^*(f)h_2(f) + h_1(f)h_2^*(f)}{S_h(f)} df, \quad (3.10)$$

where $S_h(f)$ is the PSD of the detector. The integration in the above is carried out between a lower cutoff frequency corresponding to the detector and the upper cutoff frequency, which is the frequency at which the signal terminates.

For all the ground-based detectors the upper frequency cutoff is minimum of the waveform's termination frequency (f_3) as given in Ref.[37], whereas for LISA, it is $\min(f_3, 0.1 \text{ Hz})$. We have not considered here the orbital motion of LISA and have instead treated LISA like a static detector. The orbital motion and the corresponding modulations to the waveform are likely to be more important for distance estimation and source localization which are not relevant to the present analysis. However, we note that the orbital motion of the detector would indeed be important for detection of GW signals. For both ground- and space-based detectors, we use only single detector configurations for our analysis.

Details of Fisher matrix implementation can be found in Refs [47, 48]. The errors computed from the Fisher matrix are a lower bound on the actual errors when the signal-to-noise ratio (SNR) is high and the noise is Gaussian. Since these assumptions are likely to hold, as can be seen from the right panel of Fig. 1, for most detections using advanced detectors, we believe Fisher matrix-based estimates would suffice here. One may refer to Ref. [49] for a detailed discussion on the domain of applicability of the Fisher matrix.

IV. CALCULATION OF THE BOUNDS ON DISPERSION

For our studies, we use equal-mass systems at a distance of 1 Gpc ($z \approx 0.2$) for the ground-based detectors. The right-hand panel of Fig. 1 shows a comparison of the SNRs from the future detectors. Henceforth, we shall use aLIGO to mean the improved

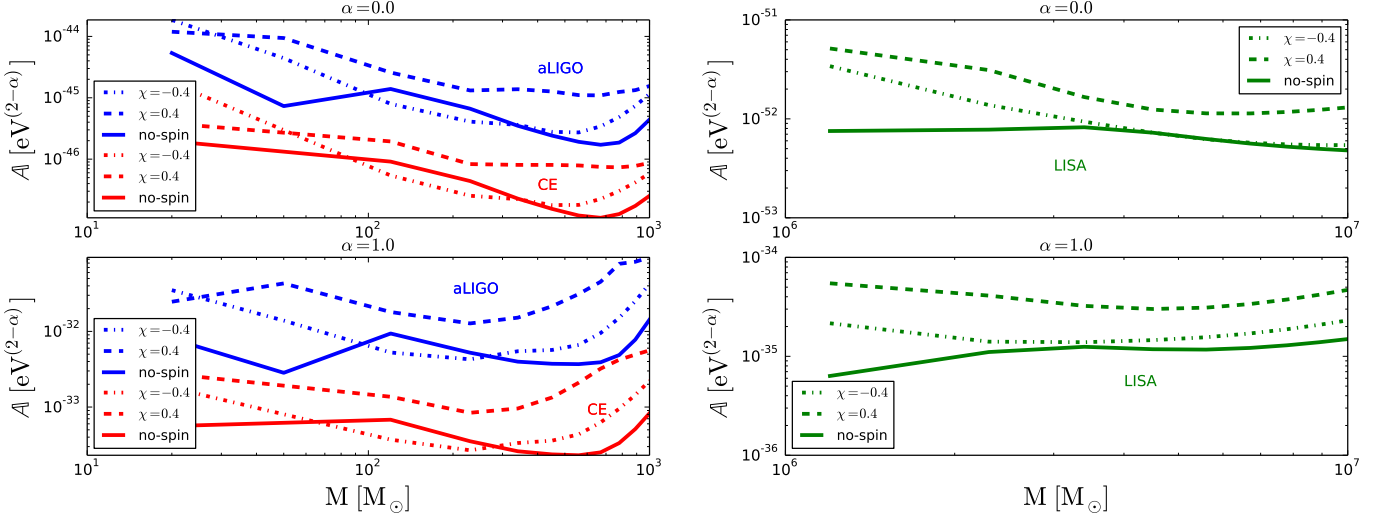


FIG. 3: Upper bounds on \mathbb{A} varying with total mass for spinning sources overlaid with nonspinning sources for CE and aLIGO (left) and LISA (right). The bounds are for $\alpha = 0$ (top panel) and $\alpha = 1$ (bottom panel). The plots are made for $\chi = 0.4$ (dashed lines), $\chi = -0.4$ (dash-dotted lines) and non-spinning sources. In general, spins deteriorate the bounds, though $\chi = -0.4$ is found to perform almost comparably with the nonspinning counterparts for higher mass sources. It is discussed in Sec. IV B.

zero-detuned-high-power aLIGOZeroDetHighPower sensitivity. For the space-based detector LISA, we use equal-mass systems located at a distance of 3 Gpc ($z \approx 0.5$). We have reproduced very closely the results of Ref.[29] for the $\alpha = 0$ case and of Ref.[15] for the corresponding α (using the waveform model of Ref.[15]). Using the model of modified dispersion described in the Introduction, the waveform model of Sec. III A, and sensitivities of advanced detectors in Sec. III B, we compute the errors on $\zeta(\alpha)$ for different α values and convert the errors $\Delta\zeta$ to upper bounds on \mathbb{A} using the expression for ζ . We compare the bounds obtained with and without the inclusion of spins in the parameter space in the next two subsections.

A. Bounds from nonspinning sources

To derive the bounds on \mathbb{A} for nonspinning binaries, we use the parameter space given by $\vec{\theta} \equiv \{\log C, \phi_c, t_c, \log M, \log \eta, \zeta\}$. For aLIGO and CE detectors, we use sources with total masses lying between 20 and 1000 M_\odot , and for the ET, we use sources with total masses lying between 20 and 3000 M_\odot . For LISA, we use total masses lying between 10^5 and $10^7 M_\odot$. These choices are motivated by the sensitivities of the detectors. Figure 2 shows the bounds for $\alpha = \{0, 1, 2.5, 3\}$ as representative cases of $\alpha < 2$ and $\alpha > 2$ for the advanced LIGO, ET, CE, and LISA detectors. In terms of broad features, one finds that as we increase α from 0 to 4 the bound on \mathbb{A} worsens very rapidly by about 54 orders of magnitude for ground-based detectors and 58 orders of magnitude for LISA. This has been known in the literature [4, 15, 16] and can be attributed to the fact that higher α induce phase corrections at higher frequencies (higher post-Newtonian orders, if one naively views the phase corrections to be post-Newtonian-like). Since gravitational-wave detectors have less capability to constrain phase deformations at higher orders [6, 8, 10], this is naturally expected.

We next note that for $\alpha = 0$ the phase deformations are degenerate with that due to a mass of the graviton, for which the upper bounds on the dispersion parameter \mathbb{A} goes as $\mathbb{A} \equiv m_g^2$. The bounds get worse with higher α . Among the ground-based detectors, ET performs better than CE though they perform comparably at sources with higher mass. The sensitivity of ET at high and low frequencies is better than CE, as can be noted from the sensitivity plot in Fig. 1 which explains why the bounds from ET are better for lower mass sources than from CE. They both outperform aLIGO by about an order of magnitude.

Bounds from LISA are much better for $\alpha = 0, 1$ than those obtained from the other detectors. For $\alpha = 0$, this is what has been observed by Keppel and Ajith [29]. However, for $\alpha > 1$, the bounds from LISA are worse compared to the ground-based detectors and they become progressively worse as we go to higher values of α . This somewhat unexpected trend may be explained by noting that the dephasing due to modified dispersion scales as $\delta\Psi \sim \mathbb{A} f^{\alpha-1}$, and hence for a given \mathbb{A} , the dephasing will be larger in the LISA band for $\alpha \leq 1$ whereas for $\alpha > 1$, dephasing will be larger for the ground-based detector band ($f \geq 1\text{Hz}$). A larger dephasing would imply better prospects for constraining the parameter \mathbb{A} , as seen in the figure.

For $\alpha = 0$, we have compared our bounds obtained on $\lambda_{\mathbb{A}}$ with that of the graviton Compton wavelength λ_g reported by Keppel and Ajith [29]. We have compared our bounds with those reported in Table III in Ref. [29] for equal-mass binaries with $f_{\text{low}} = 10$ Hz for ground-based detectors and $f_{\text{low}} = 10^{-4}$ Hz for LISA and have found reasonable agreement.

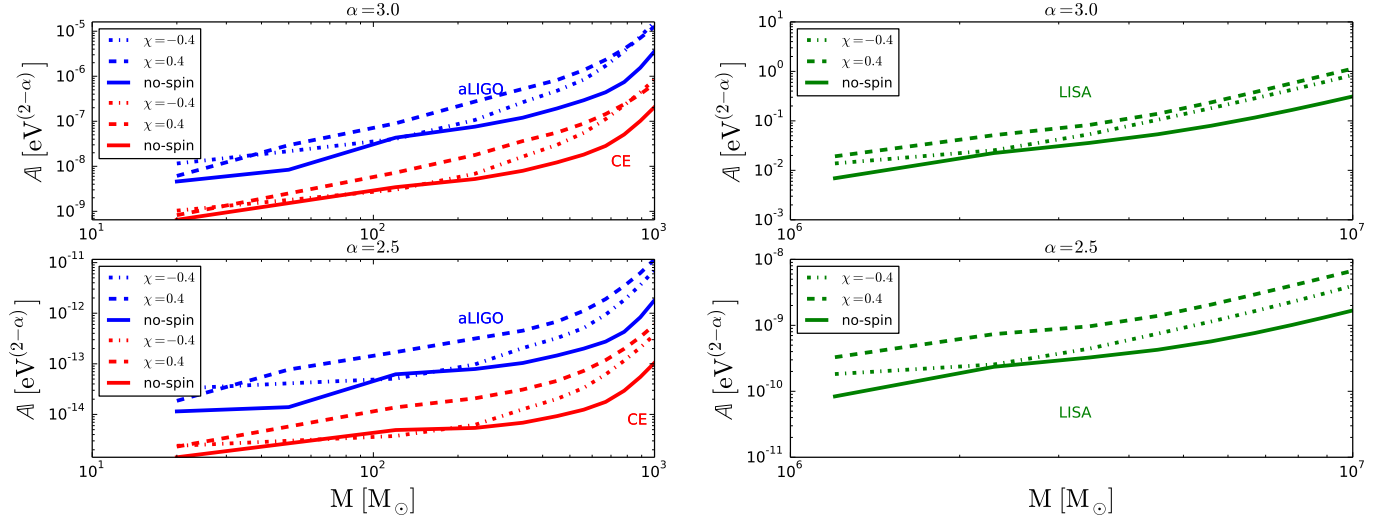


FIG. 4: Upper bounds on A varying with total mass for spinning sources overlaid with nonspinning sources for CE and aLIGO (left) and LISA (right). The bounds are for $\alpha = 3$ (top panel) and $\alpha = 2.5$ (bottom panel). The plots are made for $\chi = 0.4$ (dashed lines), $\chi = -0.4$ (dash-dotted lines), and nonspinning sources. A more detailed discussion occurs in Sec. IV B.

B. Bounds from spinning sources

For spinning sources, we include χ in our parameter set. We work with the parameter set $\vec{\theta} \equiv \{\log C, \phi_c, t_c, \log M, \log \eta, \zeta, \chi\}$. For ground-based detectors, we use sources with total masses lying between 20 and 1000 M_\odot , and for LISA, we use total masses lying between 10^6 and $10^7 M_\odot$. For the spin parameter χ , we use a Gaussian prior with a mean of 0 and standard deviation of 0.3, while calculating errors. This is motivated by the fact that in all the observed BBH mergers so far measured values of χ are small and close to zero. However we have chosen the values of $\chi = \pm 0.4$ to study the effect of spins and their alignment, which are greater than the width of the prior so that we are not severely limited by the priors. We see that the bounds in general worsen with inclusion of spins, as expected when we add a new parameter without more structure to the waveform. The inversion accuracy, defined as largest element in the difference between the identify matrix and the product of the covariance matrix with the Fisher matrix, is $\sim 10^{-3}$ for spinning sources.

Figure 3 shows a comparison of bounds from the spinning sources and the non-spinning sources for $\alpha = 0, 1$. Figure 4 shows the bounds for the same sources at $\alpha = 2.5$ and 3.

We observe the general trend that systems that have spins antialigned with respect to the orbital angular momentum yield better bounds than those of which the spins are aligned with respect to the orbital angular momentum, despite the SNRs of the former being smaller than the latter. Since we are measuring a propagation effect, the bounds are likely to improve when sources are at a larger distance. From the right panel of Fig. 1, it is evident that SNRs for the aligned spinning sources are higher than those for the antialigned sources. For a fixed source at any α , this is as if the wave travels a larger effective distance for a negative value of χ . The bound is therefore better with a larger propagation distance.

V. CONCLUSION AND OUTLOOK

As a follow up to the recent LIGO bounds on the dispersion of GWs [4], we extend some of the previous works [32, 33] to assess the capabilities of advanced ground- and space-based interferometers to constrain any possible dispersion of GWs using binary black hole observations. Our important results are summarized in Table I, which presents the typical (median) bounds on dispersion for ground- and space-based detector configurations, for various types of modification to the dispersion (different values of α). Sources for ground-based detectors are at a redshift of 0.2 (≈ 1 Gpc) whereas those for LISA are at $z = 0.5$ (≈ 3 Gpc). The numbers in parentheses denote the bounds for $\chi = 0.4$. For $\alpha \leq 1$, the bounds improve by several orders of magnitude as we go from advanced LIGO to 3G detectors to LISA. However, for $\alpha > 1$, the bounds are worse for LISA compared to ground-based detectors. In all the cases, 3G ground-based detectors can constrain GW dispersion much more stringently than second-generation detectors. As expected, inclusion of spins worsens the bounds, but the dependence of the bounds on the spins is not straightforward to understand as the waveform model we employ uses an effective spin parameter that is a linear combination of masses and spins.

\mathbb{A} [in $\text{eV}^{2-\alpha}$]				
Detector	$\alpha = 0$	$\alpha = 1$	$\alpha = 2.5$	$\alpha = 3$
aLIGO	3.50×10^{-46} (1.33×10^{-45})	4.87×10^{-33} (3.12×10^{-32})	1.46×10^{-13} (6.84×10^{-13})	1.93×10^{-7} (8.25×10^{-7})
CE	1.73×10^{-47} (8.06×10^{-47})	3.34×10^{-34} (2.10×10^{-33})	1.24×10^{-14} (7.25×10^{-14})	1.82×10^{-8} (8.91×10^{-8})
LISA	5.95×10^{-53} (1.24×10^{-52})	1.20×10^{-35} (3.75×10^{-35})	4.99×10^{-10} (2.07×10^{-9})	6.66×10^{-2} (2.36×10^{-1})
ET	5.08×10^{-48}	1.41×10^{-34}	1.52×10^{-14}	2.63×10^{-8}

TABLE I: Median of upper bounds on \mathbb{A} (in units of $\text{eV}^{2-\alpha}$) obtained over a range of masses for advanced LIGO, the Einstein Telescope, Cosmic Explorer, and LISA sensitivities, which represent second-generation, third-generation, and space-based detectors. The bounds quoted are for nonspinning systems, while the ones in brackets are bounds from systems with an effective spin $\chi = 0.4$. The sources for the ground-based detectors are assumed to be at a redshift of 0.2, while those for LISA are assumed to be at a redshift of 0.5. See Figs. 3 and 4 for details.

Acknowledgments

A.S. thanks MHRD for financial assistance. A.S. would like to thank Chennai Mathematical Institute for hospitality during the initial phase of the project. K.G.A. acknowledges Grant No. EMR/2016/005594 from Science and Engineering Research Board (SERB), India. K.G.A. is partially supported by a grant from Infosys Foundation. K.G.A. acknowledges support from the Indo-US Science and Technology Forum through the Indo-US Centre for the Exploration of Extreme Gravity (Grant No. IUSSTF/JC-029/2016). We have significantly benefited from discussions from many members of the LIGO Scientific Collaboration and Virgo Collaboration. We thank M. Agathos, S. Babak, W. Del Pozzo, A. Ghosh, C. Mishra, R. Nayak, B. S. Sathyaprakash, C. Van Den Broeck, S. Vitale for many insightful discussions. K.G.A. thanks L. Stein and A. Laddha for useful discussions. We thank Archisman Ghosh for critical reading of the manuscript and much input, which helped us improve the presentation in the draft. We thank N. V. Krishnendu for careful reading of the manuscript. Useful conversations with Stefan Hild on Einstein Telescope noise PSDs are gratefully acknowledged. This research was initiated during the Future of Gravitational Wave Astronomy Workshop at the International Centre for Theoretical Sciences (code: ICTS/Prog-fgwa/2016/04).

-
- [1] B. P. Abbott et al. (LIGO Scientific Collaboration and Virgo Collaboration), Phys. Rev. Lett. **116**, 061102 (2016), 1602.03837.
 - [2] B. P. Abbott et al. (LIGO Scientific Collaboration and Virgo Collaboration), Phys. Rev. Lett. **116**, 241103 (2016), 1606.04855.
 - [3] B. P. Abbott et al. (LIGO Scientific Collaboration and Virgo Collaboration), Phys. Rev. X **6**, 041015 (2016), 1606.04856.
 - [4] B. P. Abbott et al. (LIGO Scientific Collaboration and Virgo Collaboration), Phys. Rev. Lett. **118**(22), 221101 (2017), 1706.01812.
 - [5] K. G. Arun, B. R. Iyer, M. S. S. Qusailah, and B. S. Sathyaprakash, Class. Quant. Grav. **23**, L37 (2006), 0604018.
 - [6] K. G. Arun, B. R. Iyer, M. S. S. Qusailah, and B. S. Sathyaprakash, Phys. Rev. D **74**, 024006 (2006), 0604067.
 - [7] C. K. Mishra, K. G. Arun, B. R. Iyer, and B. S. Sathyaprakash, Phys. Rev. D **82**, 064010 (2010), 1005.0304.
 - [8] N. Yunes and F. Pretorius, Phys. Rev. D **80**, 122003 (2009), 0909.3328.
 - [9] T. G. F. Li, W. Del Pozzo, S. Vitale, C. Van Den Broeck, M. Agathos, J. Veitch, K. Grover, T. Sidery, R. Sturani, and A. Vecchio, Phys. Rev. D **85**, 082003 (2012), 1110.0530.
 - [10] M. Agathos, W. Del Pozzo, T. G. F. Li, C. Van Den Broeck, J. Veitch, and S. Vitale, Phys. Rev. D **89**, 082001 (2014), 1311.0420.
 - [11] B. P. Abbott et al. (LIGO Scientific Collaboration and Virgo Collaboration), Phys. Rev. Lett. **116**, 221101 (2016), 1602.03841.
 - [12] C. M. Will, Phys. Rev. D **57**, 2061 (1998), gr-qc/9709011.
 - [13] K. G. Arun and C. M. Will, Class. Quant. Grav. **26**, 155002 (2009), 0904.1190.
 - [14] A. Ghosh et al., Phys. Rev. D **94**, 021101 (2016), 1602.02453.
 - [15] S. Mirshekari, N. Yunes, and C. M. Will, Phys. Rev. D **85**, 024041 (2012), 1110.2720.
 - [16] N. Yunes, K. Yagi, and F. Pretorius, Phys. Rev. D **94**, 084002 (2016), 1603.08955.
 - [17] S. Kiyota and K. Yamamoto, Phys. Rev. D **92**, 104036 (2015), 1509.00610.
 - [18] V. A. Kosteleck and J. D. Tasson, Phys. Lett. **B749**, 551 (2015), 1508.07007.
 - [19] J. D. Tasson, Symmetry **8**, 111 (2016), 1610.05357.
 - [20] V. A. Kosteleck and M. Mewes, Phys. Lett. **B757**, 510 (2016), 1602.04782.
 - [21] D. Colladay and V. A. Kosteleck, Phys. Rev. D **58**, 116002 (1998), hep-ph/9809521.
 - [22] V. A. Kosteleck and N. Russell, Rev. Mod. Phys. **83**, 11 (2011), 0801.0287.
 - [23] D. Blas, M. M. Ivanov, I. Sawicki, and S. Sibiryakov, JETP Lett. **103**, 624 (2016).
 - [24] N. Cornish et al. (to be published).
 - [25] M. Puntoro et al., Class. Quantum Grav. **27**, 194002 (2010).
 - [26] B. P. Abbott et al. (LIGO Scientific Collaboration and Virgo Collaboration), Class. Quant. Grav. **34**, 044001 (2017), 1607.08697.
 - [27] K. Danzmann and the LISA study team, Class. Quant. Grav. **13**, A247 (1996).
 - [28] E. Berti, A. Buonanno, and C. M. Will, Phys. Rev. D **71**, 084025 (2005), gr-qc/0411129.
 - [29] D. Keppel and P. Ajith, Phys. Rev. D **82**, 122001 (2010), 1004.0284.
 - [30] L. Blanchet, Living Rev. Rel. **9**, 4 (2006), arXiv:1310.1528.
 - [31] L. Blanchet, T. Damour, G. Esposito-Farèse, and B. R. Iyer, Phys. Rev. Lett. **93**, 091101 (2004), gr-qc/0406012.
 - [32] D. Hansen, N. Yunes, and K. Yagi, Phys. Rev. D **D91**, 082003 (2015), 1412.4132.
 - [33] K. Chamberlain and N. Yunes, Phys. Rev. D **96**, 084039 (2017), 1704.08268.

- [34] P. A. R. Ade et al. (Planck Collaboration), *Astron. Astrophys.* **594**, A13 (2016), 1502.01589.
- [35] G. Calcagni, *Phys. Rev. Lett.* **104**, 251301 (2010).
- [36] G. Amelino-Camelia, *Nature* **418**, 34 (2002), 0207049.
- [37] P. Ajith et al., *Phys. Rev. Lett.* **106**, 241101 (2011), 0909.2867.
- [38] K. G. Arun, A. Buonanno, G. Faye, and E. Ochsner, *Phys. Rev. D* **79**, 104023 (2009), 0810.5336.
- [39] S. Khan, S. Husa, M. Hannam, F. Ohme, M. Purrer, X. J. Forteza, and A. Bohe, *Phys. Rev. D* **93**, 044007 (2016), 1508.07253.
- [40] P. Ajith, *Phys. Rev. D* **84**, 084037 (2011), 1107.1267.
- [41] S. Hild et al., *Class. Quantum Grav.* **28**, 094013 (2011).
- [42] M. Evans, R. Sturani, and S. Vitale, LIGO-T1500293 (2016).
- [43] S. E. Dwyer et al., *Phys. Rev. D* **91**, 082001 (2015), 1410.0612.
- [44] B. S. Sathyaprakash, private communication (2017).
- [45] M. Armano et al., *Phys. Rev. Lett.* **116**, 231101 (2016).
- [46] S. Babak et al., *Phys. Rev. D* **95**, 103012 (2017), 1703.09722.
- [47] C. Cutler and E. Flanagan, *Phys. Rev. D* **49**, 2658 (1994), 9402014.
- [48] E. Poisson and C. M. Will, *Phys. Rev. D* **52**, 848 (1995), 9502040.
- [49] M. Vallisneri, *Phys. Rev. D* **77**, 042001 (2008), gr-qc/0703086.